CONF-9207172--2

LA-UR- 92-1329

Title: LOW ENERGY NEUTRAL ATOM IMAGING

LA-UR--92-1329

DE92 013531

Author(s): D.J. McComas, H.O. Funsten, J.T. Gosling, K.R. Moore, and M.F. Thomsen

Submitted to: SPIE's 1992 International Symposium on Optical Applied Science and Engineering, San Diego, CA 19-24 July 1992

MASTER

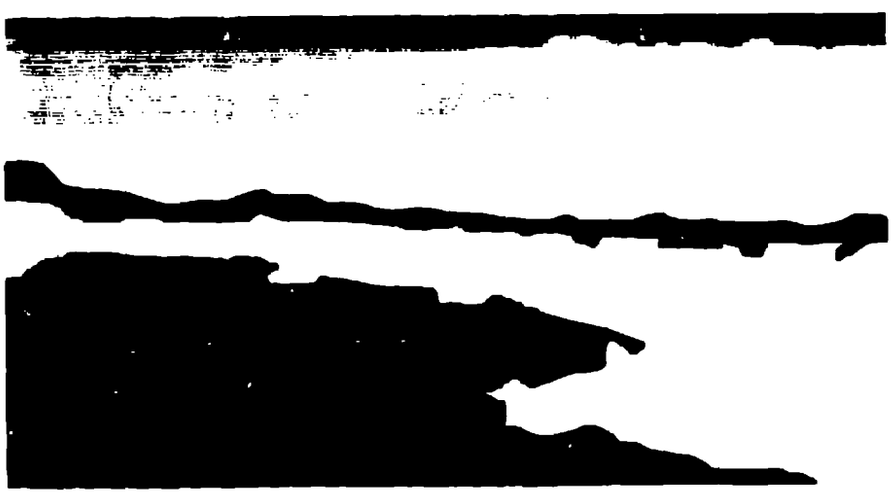

Los Alamos
NATIONAL LABORATORY

Low energy neutral atom imaging

D.J. McComas, H.O. Funsten, J.T. Gosling,
K.R. Moore, and M.F. Thomsen

Space Plasma Physics Group, MS-D438
Los Alamos National Laboratory
Los Alamos, NM 87545

ABSTRACT

Energetic neutral atom (ENA) and low energy neutral atom (LENA) imaging of space plasmas are emerging new technology which promises to revolutionize the way we view and understand large scale space plasma phenomena and dynamics. ENAs and LENAs are produced in the magnetosphere by charge exchange between energetic and plasma ions and cold geocoronal neutrals. While imaging techniques have been previously developed for observing ENAs, with energies above several tens of keV, most of the ions found in the terrestrial magnetosphere have lower energies. We recently suggested that LENAs could be imaged by first converting the neutrals to ions and then electrostatically analyzing them to reject the UV background. In this paper we extend this work to examine in detail the sensor elements needed to make an LENA imager. These elements are 1) a biased collimator to remove the ambient plasma ions and electrons and set the azimuthal field-of-view; 2) a charge modifier to convert a portion of the incident LENAs to ions; 3) an electrostatic analyzer to reject UV light and set the energy passband; and 4) a coincidence detector to measure converted LENAs while rejecting noise and penetrating radiation. We also examine the issue of LENA imager sensitivity and describe ways of optimizing sensitivity in the various sensor components. Finally, we demonstrate in detail how these general considerations are implemented by describing one relatively straightforward design based on a hemispherical electrostatic analyzer.

I. INTRODUCTION

Energetic neutral atoms (ENAs) and low energy neutral atoms (LENAs) arise from energetic particle (10s -

100s of keV) and plasma ions (few eV - 10s of keV), respectively, in the magnetosphere. These magnetospheric ions charge exchange with cold neutral atoms from the neutral geocorona to produce ENAs and LENAs which accurately reflect the local ion distributions and geocoronal densities. Since such neutrals are unaffected by electric and magnetic fields, they radiate outward with the velocities they had at the instant of charge exchange. Remote imaging of these neutrals provides line-of-sight integrated observations of the magnetospheric energetic particle[a,b] and plasma ion populations[c].

In this paper we discuss implications of, and describe one technique in detail for low energy neutral atom imaging. In this section we describe the importance of LENA imaging for space plasma physics in general and terrestrial magnetospheric physics, in particular. We then go on to discuss the primary physical problem with carrying out such LENA measurements and suggest a number of possible solutions. In section 2 we examine the components of one particular type of LENA imager which is technically well enough developed for immediate space flight. In this section we also discuss each of the building blocks of such an imager in turn and examine various ways of optimizing each for overall sensor sensitivity. In section 4 we provide an example design for a simple LENA imager in more detail and discuss other possible designs which would provide even higher sensitivity. Finally, in section 5 we summarize this work.

1.1 The potential scientific return from LENA imaging

Magnetospheric imaging with charge exchange neutrals promises to be a critical new technique for examining the global morphology and dynamics of the terrestrial (and planetary) magnetospheres as well as other space plasmas. The present state of knowledge of magnetospheric physics has been gleaned from *in situ* observations from one or occasionally several spacecraft. While such observations provide excellent and detailed information about the local plasma and field environments, they do not provide simultaneous information across the magnetosphere. In contrast, magnetospheric neutral imaging will provide somewhat less detailed information, but with synoptic coverage of the magnetospheric environment.

Higher energy ions (that produce ENAs) are abundant in the inner portions of the terrestrial ring current. However, throughout the remainder of the magnetosphere, lower energy plasma energy ions (that produce LENAs) are predominant. Regions that are uniquely populated by lower energy plasmas include the outer ring current and dayside extension of the plasma sheet, the plasma sheet proper, and the magnetosheath. In addition, charge exchange between magnetospheric ions and the geocoronal neutrals has a larger

crc sssection at lower energies. For example, the crosssection between H^+ and cold neutral hydrogen in the geocorona drops by a factor of ~3 (CHECK) between 1 keV and 10 keV and ~10 (CHECK) between 1 and 100 keV. As a consequence, most of the magnetosphere radiates higher fluxes of LENAs than ENAs[c,d], and LENA imaging provides for remote observation of the magnetosphere which is both qualitatively and quantitatively unachievable with higher energy, ENA imaging.

Figure 1 displays a greyscale simulated image of the terrestrial magnetosphere observed in 5 keV LENAs from 9 R_E in the +Y GSE direction. The details of this simulation are given by Moore et al.[d]. The Earth is in the center of the plot with an azimuthal angle (in the GSE X-Y plane) of 180°; the horizontal axis is the colatitude polar angle. The brightened symmetric region surrounding the Earth is produced by the stormtime ring current while the horizontal bright structure extending to the right of the Earth is the plasma sheet.

Scientific targets for LENA imaging of the terrestrial magnetosphere include the plasma sheet, ring current and dayward extension of the plasma sheet, the magnetopause, and the magnetosheath. It is clear from Figure 1 that if the plasma sheet can be imaged in LENAs, many important magnetospheric questions could be unambiguously answered. Such questions include: 1) how does the plasma sheet thickness and location vary as a function of time and substorm phase? and 2) does reconnection sever and eject part of the plasma sheet, and if so when and how much? Another example of important observations that may be addressable from a global viewpoint for the first time is the dynamics of the magnetopause. Since the magnetopause is a compositional boundary, and since both hydrogen and oxygen can be unambiguously imaged, it may be possible to study the dynamics of the global magnetopause shape and location for the first time.

1.2 The difficulty with and approaches for LENA imaging

The primary technical problem with observing LENAs in space is that such observations must be made against a large Ly-α ultra violet (UV) background. Typical UV fluxes of $>10^{10}$ cm $^{-2}$ s $^{-1}$ are scattered from the Sun by hydrogen atoms in the geocorona[e]. Low energy detectors such as channel electron multipliers (CEMs) and microchannel plates (MCPs) are sensitive to UV photons so that such large backgrounds swamp any LENA signal in bare low energy detectors. In order to image the low fluxes of LENAs in the magnetosphere the UV background must be somehow rejected.

At higher energies, ENA detectors proposed to date have relied on relatively thick (~15 $\mu g/cm^2$) carbon foils to screen out almost all of the UV[f]. Subsequent time-of-flight or coincidence measurements of the passed neutrals are then used to differentiate ENAs from any transmitted UV photons. Unfortunately such thick foils cannot be used with LENAs (below several tens of keV) due to the large energy straggling and angular scattering. In order to effectively detect LENAs, methods must be found which do not rely on relatively thick foils to attenuate the UV.

In theory, UV rejection, and hence effective LENA detection, can be achieved either directly or indirectly. Direct detection of the LENAs would be accomplished by filtering out the UV light background and directly detecting the LENAs on a low energy detector. Such filtering might be accomplished, for example, with nuclear track filters[g] or by some other means. Any such technique, however, would need to reject UV photons to an extremely high level (~10^{10}:1) while still providing a large throughput for LENAs. A number of these techniques are presently under study and UV filtering may ultimately prove to be an excellent method for LENA imaging.

Indirect detection is a fundamentally different process wherein the LENAs are modified in some way so that they can be removed from the path of the UV light rather than removing the UV from the path of the LENAs. While modifications can be accomplished via a variety of interactions, the only LENA imaging technique that has been well developed so far relies on charge state modification (ionization) in an ultra-thin foil (< 0.5 $\mu g/cm^2$) followed by electrostatic analysis of the newly ionized LENAs[c]. A non-imaging, thicker foil implementation of this detection technique was actually flown on a sounding rocket in 1970[h]. Unfortunately, the limited observations from this experiment were never unambiguously interpreted.

2. LENA IMAGER DESIGN

2.1 LENA Imager Components

The four basic components of the LENA imaging approach described by McComas et al.[c] are shown schematically in Figure 2 and summarized in Table 1. The neutrals first enter the imager through a collimator section which has either high voltage and ground or positive and negative high voltages applied alternately on the collimator plates. Entering ions below some critical energy are deflected into the collimation plates

and thereby rejected. At higher energies some ions will pass the collimator, however if this cutoff energy is sufficiently high, the transmitted ions will be too energetic to pass the subsequent electrostatic analyzer. For the several degree angular resolutions typically sought for neutral imagers, ions with energies per charge (E/q) as large as several hundred keV ran be readily swept out using collimator voltages of only several kV.

Immediately following the collimator is the ionization or charge state conversion section of the sensor. While several other means of ionization are presently under study, the best presently developed method for space plasma imaging applications is an ultra-thin (<0.5 $\mu g/cm^2$) carbon foil which modifies the charge state of some fraction of the incident LENAs. Since the LENAs are traveling slowly compared to the Bohr velocity, they effectively come into equilibrium with the foil material during their transit through the solid. Consequently, the exit charge state distribution is independent of the entrance charge state and rather depends simply upon the material properties of the foil material and the LENA. Figure 3 summarizes the positive ion conversion efficiency for the dominant magnetospheric LENA species, hydrogen, as a function of energy[i]. Note that this ionization efficiency is sufficiently large that a substantial fraction of all LENAs passing through the collimator and into the sensor can be detected at all energies in the LENA range of interest.

Subsequently to ionization, electrostatic analysis deflects the particles both to reject the UV photons and to provide energy information about the LENA distributions. Electrostatic analyzers have been flown in space to characterize the plasma environment on many missions since the early 1960s and this method has, in fact, been the mainstay of space plasma observations. An electrostatic analyzer is comprised of a set of curved analyzer plates between which an electric field is produced. Trajectories of charged particles within the energy and angle passband of the analyzer are bent by the electric field in such a way that they pass between the plates. Charges particles outside of this passband strike either the inner or outer plate and are rejected. While generally heavier, magnetic and combined electric/magnetic analyzers could also be employed for deflecting the ionized LENAs.

Transmitted ions are detected behind the exit gap of the electrostatic analyzer. In order to provide a high signal to noise ratio and reject the background caused by penetrating radiation, time-of-flight (TOF) or coincidence measurements are required. TOF measurements have the advantage that they provide unambiguous information about the ion species being detected. Because the vast majority of the LENAs observable in the terrestrial magnetosphere are hydrogen, with some smaller component of oxygen, it is not necessary to make high resolution TOF measurements. Rather, differentiation between hydrogen and

oxygen is achievable with a low resolution TOF which simply sorts the delays into longer and shorter intervals; under highly constrained resources even simple coincidence circuitry is sufficient to make good (albeit non mass resolved) neutral images.

Table 1. Elements of an LENA Imager

Component	Function
1. Collimator	removes ambient plasma ions and electrons and sets azimuthal field-of-view
2. Charge modifier	converts a portion of the incident LENAs to ions
3. Electrostatic analyzer	rejects UV, electrons, and ions outside passband; sets energy resolution
4. Coincidence detector	detects converted LENAs while rejecting noise and penetrating radiation

While an LENA imager of the type described here has never been flown before, all four of the components which comprise it have substantial flight histories. As a consequence,we believe that there can be little doubt that LENA imaging with instrumentation described here is a mature space sensor technology which is fully flight ready.

2.2 LENA Imager Sensitivity and Geometric Factors

Just as for in situ space plasma analyzers the geometric factor, G, sets the basic sensitivity of an LENA imager for detecting particles. The geometric factor is a measure of the instrument's aperture area, A; energy selectivity $\Delta E/E$; azimuthal angular selectivity $\Delta\alpha$; and overall detection efficiency, ε. G is defined (after Gosling et al.[3])

$$G = 2 A \varepsilon <\Delta\alpha \Delta E/E> \quad (1)$$

and is commonly given in units of cm^2 sr eV/eV. The peak count rate, C, observed by an analyzer for a given flux of LENAs, J_{LENA}, is

$$C = G J_{LENA} E \quad (2)$$

Whole instrument geometric factors for typical *in situ* magnetospheric plasma analyzers range up to ~0.01

cm^2 sr eV/eV. For typical storm time ring current and plasma sheet LENA fluxes of 1000 and 50 displayed in Figure 1, peak count rates of 50 and 2.5 s^{-1} would be achieved for a single energy measurement from an imager staring at these structures. A geometric factor of ~1 cm^2 sr eV/eV (full instrument), while appreciably larger than currently flown plasma instrumentation, is an achievable and appropriate goal for a high sensitivity LENA imager. In order to achieve such a large geometric factor, and hence an imager's sensitivity for measuring LENAs, the four instrument components identified above must each be optimized.

It is evident from equation 1 that the geometric factor of an LENA imager is set by the aperture area, angular and energy acceptance, and overall efficiency. An aperture area of several cm^2 is an essential starting point if a large overall geometric factor is to be achieved. Charge state conversion efficiency must also be maximized since only that fraction of the incident LENAs that is ionized in the foil can be subsequently detected. Typical ultra-thin carbon foil conversion efficiencies measured at Los Alamos range from ~6% at 1 keV to ~40% at 30 keV for hydrogen[1] as shown in Figure 3.

The basic G-factor for the electrostatic analyzer, which determines the energy/angle passband of the sensor, is set by the analyzer bending angle and analyzer constant , k. This analyzer constant is simply the ratio of the average analyzer radius to the analyzer gap and typical k-factors run from <10 for hot plasma analyzers to ~40 for solar wind ion analyzers. Large geometric factors are achieved by analyzers that have small k's and hence large energy and azimuthal angular acceptances. That is, the energy and azimuthal acceptances are coupled so that a high-k analyzer of a given size will have narrow energy and angular acceptances and a low G-factor while a low-k analyzer of about the same size will have comparatively broader energy and angular acceptances and a larger geometric factor.

While only rough knowledge of the energy distributions is required in hot magnetospheric plasmas, rather fine (i.e., several degree) angular resolution is needed if the magnetosphere is to be well imaged from almost any orbital vantage point. The combination of broad energy resolution, fine azimuthal angular resolution, and a very large geometric factor is most readily achieved by combining a low-k analyzer with a tight angular collimator ahead of it. This combination provides good angular resolution while still maintaining broad energy resolution and a large geometric factor.

While the geometric factor of the imager determines the overall sensitivity for detecting LENAs, the signal to

noise ratio, S/N, determines the instrumental noise background. If the sensor has a good S/N, even low flux intervals can be imaged simply by increasing integration time. If, however, the S/N ratio is poor, time integrations do not improve the observations. Consequently, it is critical to provide a high S/N for LENA imagers owing to the very low LENA fluxes. Background counting rates in MCP detectors are typically ~0.5 cm^{-2} s^{-1} while backgrounds due to penetrating radiation are highly variable and dependent on orbital location.

An anticoincidence shield around the MCP detector effectively removes most of the background due to penetrating radiation but does nothing for the intrinsic MCP dark counting or internally produced secondary electrons; this approach is generally not recommended for LENA imaging. Coincidence and TOF measurements utilize electrons ejected from a thin carbon foil to provide a start signal in combination with the MCP stop pulse. Such measurements typically have background rejection rates 10^3 - 10^4 times better than simple MCP detectors. TOF provides the additional advantage of uniquely determining the LENA species, however, the electronic circuitry required to implement TOF is more substantial than for simple coincidence. Finally, double coincidence can be implemented with some additional mechanical and electronic complication. Such measurements are generally not needed or justifiable for LENA imagers. The efficiency of a bare MCP detector for 10-20 keV (postaccelerated) ions is ~0.9. A well designed TOF or coincidence section utilizes a thin carbon foil with an exit surface electron ejection efficiency also of ~0.9 riding on a high transmission grid (> 0.9) and two MCP detectors. A total efficiency for such a section can be as high as ~0.65 which we consider to be a good trade for a 10^3-10^4 improvement in signal/noise.

2.3 Observation strategies

Spinning spacecraft have a great advantage for making LENA images of the magnetosphere since a simple fan-shaped field-of-view (FOV) can be used to sweep all or nearly all of 4π sr. This technique is already the standard for making *in situ* plasma measurements. While hot plasma observations from non-spinners are achievable with electrostatic elevation analyzers[n], neutrals cannot be deflected until they are ionized. The primary problem with spinning spacecraft is that they have a small duty cycle for observing in any given direction. Count rates in Equation 2 for an LENA sensor are reduced by the ratio of the azimuthal angular width to a full spin; this ratio is typically a few degrees to 360 or ~0.01.

Another critical factor in the effective sensitivity of an LENA imager is its energy resolution and range. For

example, an instrument that takes 10 contiguous energy cuts has a 0.1 duty cycle for any given energy. This fraction must also be multiplied into equation 2. Since the magnetospheric plasma ions are quite hot in general, we believe that only four or five energy bands covering the range of ~1-40 keV is about optimum for LENA imagers at the present state of development.

4. EXAMPLE DESIGN FOR AN LENA IMAGER ON A SPINNING SPACECRAFT

As an example of a specific LENA imager design this section will describe an imager based on a simple 180 degree bending angle spherical section analyzer (hemispherical analyzer). The basic geometry is displayed schematically in Figure 4. The electrostatic analyzer has inner and outer plate radii of 8 and 12 cm, respectively, giving an analyzer constant, k, of 2.5. The intrinsic (non collimated) azimuthal angular passband of such an analyzer is ~-26.5° to +18.5° about a normal to the aperture and the energy resolution, $\Delta E/E$, is ~25%.

The intrinsic aperture area is the product of the analyzer gap (4 cm) and its length. For an aperture length of 2 cm the aperture area is 8 cm^2. If polar angular viewing is limited to +/- 60° , then the geometric factor of this bare electrostatic analyzer is ~1 cm^2 sr eV/eV. In order to determine the LENA imager G-factor, this analyzer only G must still be reduced by 1) the neutral to ion conversion efficiency, various inefficiencies in ion transmission, and the coincidence detection efficiency, and 2) the effect of the collimator on the energy/azimuthal angular passband. Typical transmission inefficiencies that reduce the overall geometric factor of LENA imagers are summarized in Table 2.

Table 2. Transmission Efficiencies

Component	Efficiency	Source
Collimator	0.96	0.2 mm plates with 5.0 mm spacing
Grid for foil #1	0.70	333 lpi Ni electroformed mesh
Foil #1 conv eff	$.C_H$	~0.05 - 0.45
Acc. grid	0.90	70 lpi
Grid for foil #2	0.90	70 lpi with 1.0 Ni foil
Foil #2 elec emission	0.9	nominal value
CEM #1 eff	0.9	nominal value

CEM #2 eff	0.9	nominal value

Overall Efficiency:	0.40 C_H	

Collimation requirements depend on the angular resolution needed. Six degree (+/-3°) resolution, for example, can be accomplished with a stack of 9.5 cm long collimator plates with 0.5 cm spacing. If these plates are alternately biased at 5 kV and ground, ions and electrons with energies up to ~100 keV will be swept out before they can reach the aperture, rejecting all ambient ions in the LENA energy range. For 180° bending angle analyzers the energy passband is little effected by angular collimation so that the reduction in G by the collimator is simply scaled from the azimuthal angular response which is typically roughly triangular. This amounts to a factor of about 1/4 for the analyzer/collimator combination described here. Combining this reduction with the overall efficiency from Table 2 gives a whole instrument G of ~0.1 C_H cm^2 sr eV/eV.

If the charge state conversion foil is floated at +10 kV, then all exiting positive ions will have at least 10 keV of energy. This post-acceleration shifts the energy ranges that need to be covered by the electrostatic analyzer, making it possible to cover a large energy range with relatively few energy steps. The first column in table 3 displays five energy passbands that could be used to cover the entire LENA range if interest for magnetospheric plasmas. The second column gives the positive analyzer voltages that would have to be applied to the outer hemispherical plate in order to select the stated passbands. The last two columns of Table 3 give the typical ionization fractions and final calculated geometric factors for each of the five energy passbands.

Table 3. Energy Passbands and Geometric Factors

Energy passband [keV]	$V_{analyzer}$ [kV]	C_H	G-factor [cm^2 sr eV/eV]
0.8 - 4.5	6.5	0.09	0.009
4.5 - 10	8.8	0.18	0.018
10 - 17	12	0.26	0.026
17 - 26.5	16	0.36	0.036
26.5 - 40	22	0.41	0.041

5. DISCUSSION

The spherical section analyzer shown as an example (Section 4) can be easily adapted to LENA imaging and would provide reasonable sensitivity within a limited sensor mass budget of only a few kg. Such a design would provide excellent LENA imaging capability for a small explorer class mission. More advanced LENA designs based on other analyzers, such as spherical[o] and toroidal top-hat[p] analyzers[c] while somewhat larger and heavier can achieve even appreciably larger geometric factors (~1 cm^2 sr eV/eV). In addition, such analyzers provide twice the duty cycle for any given angular and energy resolution since they make simultaneous observations around an entire 360° FOV. From a somewhat less resource constrained platform, such as NASA's Inner Magnetospheric Imager (IMI) mission which is presently under study, very high sensitivity LENA observations would be achievable.

In this paper we described a space sensor technology appropriate for imaging the low energy neutral atoms emitted by the terrestrial magnetosphere and other space plasmas. Our approach is based on four sensor elements: 1) a biased collimator to remove the ambient plasma ions and electrons and set the azimuthal field-of-view; 2) a charge modifier to convert a portion of the incident LENAs to ions; 3) an electrostatic analyzer to reject UV light and set the energy passband; and 4) a coincidence detector to measure converted LENAs while rejecting noise and penetrating radiation. Since our LENA imager design is a simple combination of these elements, and since all of these elements have proven flight histories, there can be little doubt that LENA imaging technology is technically mature. The scientific return of such routine imaging of the magnetosphere would be clearly be enormous.

6. ACKNOWLEDGMENTS

This work was conducted under the auspices of the United States Department of Energy.

7. REFERENCES

a. Roelof, E.C. (1987) *Geophys. Res. Lett.*, **14**, 652-655.

b. McEntire, R.W. and D.G. Mitchell (1989) *Geophys. Monograph Ser.*, **54**, 69-80.

c. McComas, D.J., B.L. Barraclough, R.C. Elphic, H.O. Funsten III, and M.F. Thomsen (1991) *Proc.*

Natl. Acad. Sci. USA, **88**, 9598-9602.

d. Moore, K.R., D.J. McComas, H.O. Funsten, and M.F. Thomsen, this issue.

e. Rairden, R.L., L.A. Frank, and J.D. Craven (1986) *J. Geophys. Res.*, **91**, 13613-13630.

f. Hsieh, K.C., E. Keppler, and G. Schmidtke (1980) *J. Appl. Phys.*, **51**, 2242-2246.

g. Gruntman, M.A. (1991), *Proc. SPIE Internl. Symp.*, 1549, 385.

h. Wax, R.L., W.R. Simpson, and W. Bernstein (1970) *J. Geophys. Res.*, **75**, 6390-6393.

i. H.O. Funsten, D.J. McComas, and B.L. Barraclough, this issue.

j. Gosling, J.T., M.F. Thomsen, and R.C. Anderson (1984) *Los Alamos Manuel*, LA-10147-M.

n. Bame, S.J., R.H. Martin, D.J. McComas, J.L. Burch, J.A. Marshall, and D.T. Young (1989) *Geophys. Monograph Ser.*, **54**, 441-452.

o. Carlson, C.W., D.W. Curtis, G. Paschmann, and W. Michael (1983) *Adv. Space Res.*, **2**, 67.

p. Young, D.T., S.J. Bame, M.F. Thomsen, R.H. Martin, J.L. Burch, J.A. Marshall, and R. Reinhard (1988) *Rev. Sci. Instrum.*, **59**, 743-751.

Figure Captions

Fig 1. Simulated LENA image of the magnetosphere taken from 9 R_E in Y (GSE). The image shows both a storm-time ring current and a 5 keV, 0.1 cm^{-1} plasma sheet. Details of the simulation are given in Moore et al.[d].

Fig 2. Schematic summary of the four sensor elements used in our LENA imaging approach: 1) a biased collimator; 2) a charge state conversion foil; 3) an electrostatic analyzer; and 4) a coincidence or TOF detector system.

Fig 3. Measured H^+ ionization yield for hydrogen as a function of energy. Details of these measurements are given in Funsten et al.[i].

Fig 4. Scale drawing of one possible simple LENA imager based on a hemispherical electrostatic analyzer.

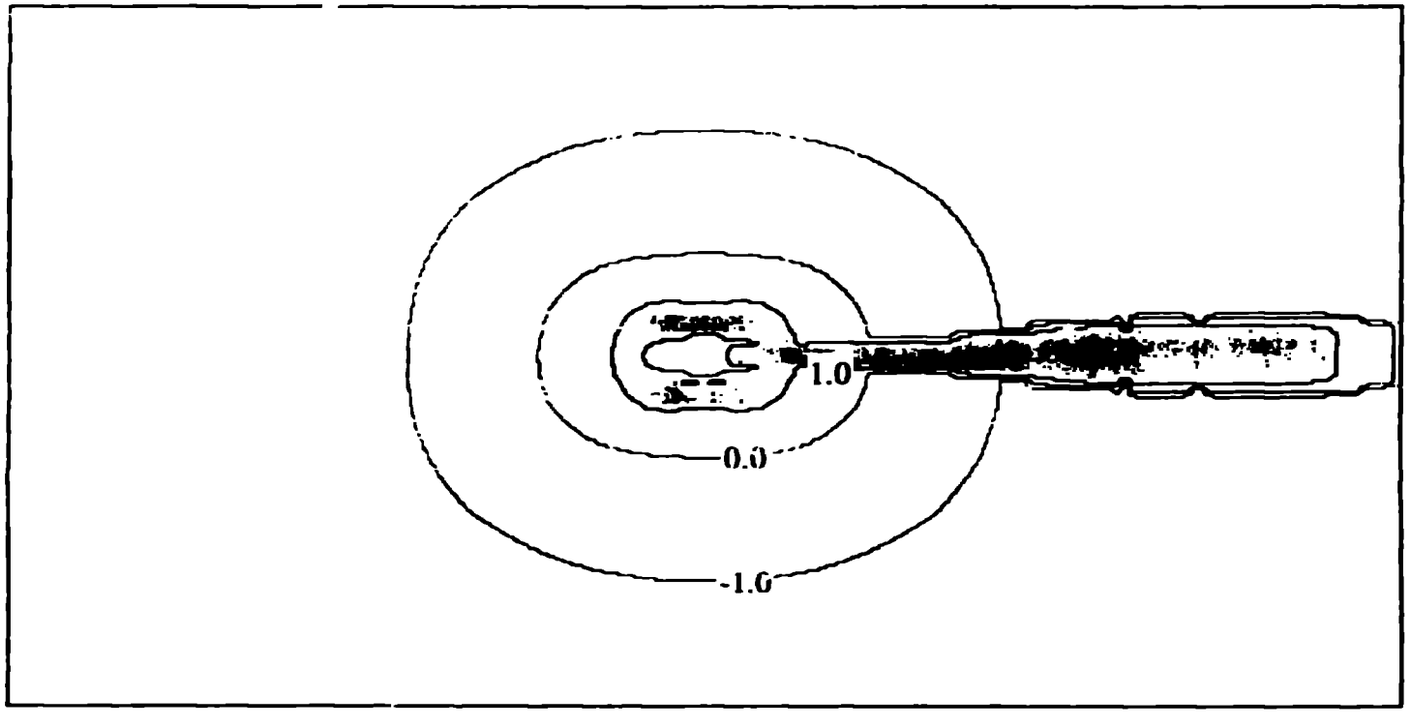

imi1_quiet_spg_vs_(row, col)

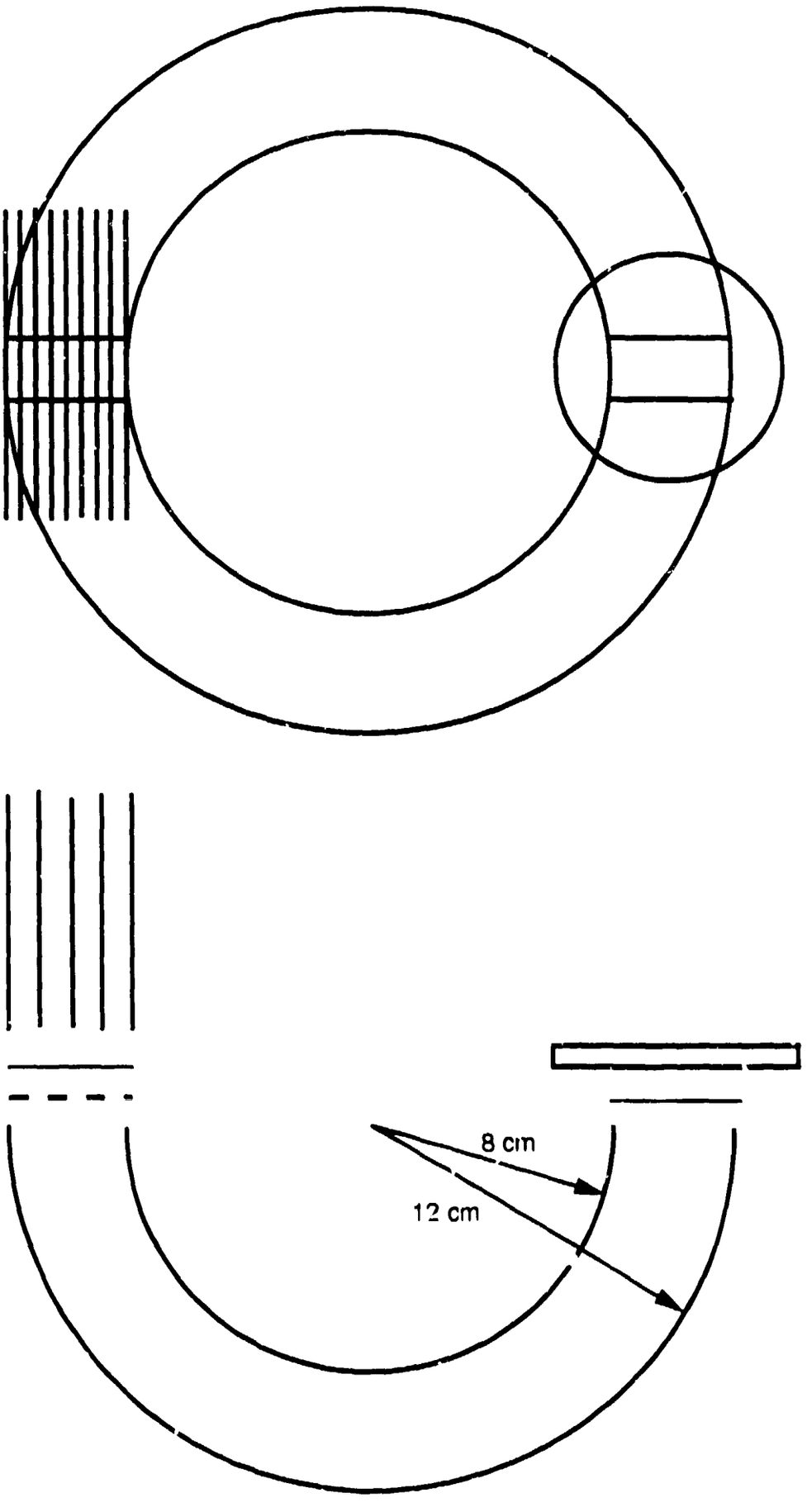
8 cm
12 cm